THE INFLUENCE OF THE GEOMETRIC PARAMETERS AND ADDITIVES ON THE FLOW AROUND AEROFOILS AND WINGS

Rafael Paulino de Queiroz, rafaelenm@yahoo.com.br
University of Brasilia

Ricardo Caiado Alvarenga, ricalvarenga@gmail.com
University of Brasilia

Francisco Ricardo da Cunha, frcunha@unb.br (Corresponding Author)
University of Brasilia

Abstract. *In this article a study on the influence of the geometric parameters and particle additive on typical aerodynamics flows is presented. A two-dimensional boundary integral method is used in order to simulate the potential flow around complex aerofoils with several thickness and camber lines. In particular, the method is applied to explore the effect of high-lift devices. In order to verify the influence of the taper ratio, geometric twist, aerodynamic twist and swept angle, the lifting-line theory, vortex-lattice method and a three-dimensional boundary integral method are used to simulate potential flow around wings. In addition, an experimental investigation was carried out in a Low-Speed Wind Tunnel to evaluate the aerodynamic characteristics of the NACA 0012, NACA 2412 and Eppler 423 aerofoils. Firstly an aerofoil is tested with a Gurney flap attached to the trailing edge in the absence of plain flap. Secondly a second aerofoil is examined by using a configuration with plain flap. Two wings with different aspect ratio are investigated. In order to control the induced drag, several configurations of endplates are tested on the wings. Results of polymer additives changing the streamline patterns of the flow around an aerofoil are also shown. It is seen that the presence of the macromolecules produce flow stabilization as a direct consequence of the variations in the distribution and intensity of vorticity in the boundary layer and the wake. In general, the numerical simulations are compared with experimental data and a very good agreement is observed.*

Keywords: *Panel method, Boundary integral method, Lifting-line theory, High-lift devices, Drag reduction*

1. INTRODUCTION

The aeronautical project is being constantly modifying with technological innovations in the scope to maximize results, as capacity of load, characteristics of performance and mainly in reduction of the manufacture and maintenance costs. This factors have total dependence on the aerodynamic characteristics thus influencing in the project of the wing. Being thus, they basically affect in the performance of landing and take-off, speed of cruise and stability and control of an aircraft.

In the research of the aerodynamics, the engineers of the aeronautical industry as Resende (2004) are constantly searching and applying new relative concepts in order to improve the performance of aerofoils.

The project of a wing can be done based on the potential flow theory. The preliminary project could be carried out through a panel bidimensional method with multi–elements ([Alvarenga, 2000]).One three-dimensional panels methods could be used to evaluate interference aerodynamics between the components of the aircraft, as fuselage and wing. A full analysis could be carried out by using the Navier-stokes equation as suggested for Carrannanto *et. al* (1998) or even though experimental measurements in wind tunnel as those carried by Rae and Pope (1984), including the use of high-lift devices that modify the geometric form of the aerofoils.

Currently, the resources more used for increasing of the efficiency in the relation drag-lift are flap, slats and slots as discussed by Mises (1959). However, such resources are constantly being adapted to the news requests of the aeronautical market. Considering that the devices to high–lift classics are extremely important with the performance of the aircraft at take-off moments and landing, the same ones deserve attention in its project due to the complexity of construction. With the objective to optimize the performance of aerofoils, researches current have invested in investigate on simple high-lift devices configuration as Gurney Flaps ([Wang and Li, 2002]). In addition high-lift devices, theoretician-experimental studies of the phenomena of the drag reduction for anisotropic particle additive has been carried out through for internal flow. Andreotti (2004) introducing a volume fraction of 350 ppm of polyacrylamide (PAMA) observing a reduction around 65% in the friction factor of the flow ([Cunha and Andreotti, 2007]). Current studies tend to verify the utilization of this polymer in external flows with the objective to verify the reduction of the formed vortex, and for being used in the nature as mechanism of protection of observed gusts of wind in biggest trees.

In the analysis of flow in finite wing, it appears the necessity of controlling the drag for geometric parameters of the wing with swept, taper ratio, geometric and aerodynamics torsion. Elements are inserted in its extremity, where these resources are used with the objective to minimize this emission of the vortex in the extremity of the wing, where the studied ones are endplates for subsonic flows and winglet for transonic. Considering the cost to implement this

devices in experimental analysis, current studies are lead using the potential flow by using various theories tools. They are frequently useful, because exist good agreement with real flows. This fact combined with their geometric generality and low computational cost, has made numerical potential flow methods a great design tools in several applications ([Alvarenga and Cunha, 2006]).

In this context, the objective of the present study was carried out to tests with variations of the aerodynamic properties of airfoil and wing by means of modifications in the geometries using experimental and numerical approaches.

2. THEORETICAL DESCRIPTION

The non-dimensional Navier-Stokes equation for the description of the of Newtonian, homogeneous, isotropic and incompressible fluid, with specific mass and viscosity constant may be expressed by:

$$\frac{\partial \tilde{\mathbf{u}}}{\partial \tilde{t}} + \tilde{\mathbf{u}} \cdot \nabla \tilde{\mathbf{u}} = -\nabla \tilde{p} + \frac{1}{Re} \nabla^2 \tilde{\mathbf{u}} \tag{1}$$

where $\tilde{p} = p/\rho U_\infty^2,\ \tilde{\mathbf{u}} = \mathbf{u}/U_\infty,\ \tilde{\mathbf{x}} = \mathbf{x}/L,\ \tilde{t} = tU_\infty/L,\ Re = \rho U_\infty L/\mu.$

In the flows with the $Re \gg 1$, typically as it occurs in flows around cylinders and aerofoils, we can write the Navier equations–Stokes less the viscous terms. From this physical condition, the scale of the hydrodynamics forces will be, $F_h \sim \rho U_\infty^2 L^2$. This analysis show that in this condition, the intensity of the hydrodynamics forces varies with $(U_\infty L)^2$, being bigger than the viscous flow that vary with (U_∞). Motivated by this fact, will be described the potential theory ([Alvarenga, 2000]). This theories will be used to compare with the experimental results in the wind tunnel.

2.1 Panel methods 2D

The bidimensional Panel methods, consist of singularity distribution of vortex in the surface the aerodynamic body. It is determined intensity of these singularity so that the boundary condition of impenetrability in the surface body will be satisfied. This method is based on the overlapping of the riots of flow produced by all the singularity in each point of body surface. These riots are propagated for inertia mechanism and gradients pressure of the flow. Beyond the condition kinematics impenetrability also exist the Kutta condition, that it establishes stagnation point in the trailing edge. The figure (1) shows to the schematic adopted by the method.

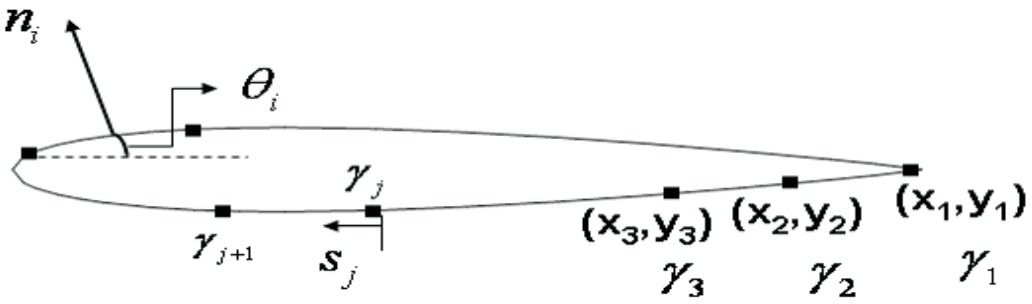

Figure 1. Sketch of coordinate system adopted for the method.

Considering a point P in the control point a panel i (in center panel) and the contribution of the velocity not disturbed flow (with one angle of inclination in relation to the line of the airfoil chord), as well as the contribution of all panels j,the velocity potencial in the control point i may be expressed as follows ([Anderson, 1991]):

$$\phi(x_i, y_i) = U_\infty (x_i \cos\alpha + y_i sen\,\alpha) - \sum_{j=1}^{m} \int_j \frac{\gamma(s_j)}{2\pi} \tan^{-1}\left(\frac{y_i - y_j}{x_i - x_j}\right) ds_j \tag{2}$$

For the present method the singularity intensity varies linearly throughout each panel, $\gamma(s_j) = \gamma_j + (\gamma_{j+1} - \gamma_j)\frac{s_j}{S_j}$, where s_j is the distance measured from the start of the panel until the end of the same, and S_j is the length of the panel j. These singularity are calculated by using the method of gauss elimination.

Having the intensities of distribution of vortices for unit of length, it can be determined the velocities in each control point through the derivative in the tangential direction of the velocity potencial that is given by:

$$U_i = \frac{\partial}{\partial s_i} \left[\phi(x_i, y_i)\right] \tag{3}$$

With the tangential velocity in each control point i, we can find the pressure distribution applying the Bernoulli equation. The experimental results will be compared with this method for simple geometries and aerofoils with flap. More details can be find in the work developed by Alvarenga (2000).

2.2 Lift line theory

The classic lift line theory is used for the analysis of flows around finite wings for potential incompressible flows, where the code uses the wing represented by the general lift distribution throughout the span. The distribution of circulation throughout the span is represented by a Fourier series of sine, namely (Anderson, 2001):

$$\Gamma(\theta) = 2bU_\infty \sum_{n=1}^{\infty} A_n sin(n\theta) \tag{4}$$

where the terms A_n are the coefficients of the Fourier series, that are determined from the numerical simulations by using the Gauss elimination method too. The remaining terms are parameters of the wing geometry and the flow. For the calculation of the global lift coefficient of the wing, the distribution of circulation eq. (4) is integrated throughout the span resulting in:

$$C_L = \frac{\pi b^2}{S} A_1 \tag{5}$$

Now, the emission of vortex generated in the tip of wing, results in on unbalancing of pressure distribution throughout the span and consequently am the induced drag. The calculation of the induced drag coefficient can be express for (Anderson, 1991):

$$C_{D,i} = \frac{C_L^2 S}{\pi e b^2} \tag{6}$$

where $e = \left(1 + \sum_{n=2}^{N} n(A_n/A_1)^2\right)^{-1}$ is the efficiency factor of the wing and considered 1 for elliptical the plan wing. It is important to notice that lift distribution that results the minor induced drag is the elliptical distribution. The prediction from this theory will be compared with the experimental results.

Considering the difficulty of manufacturing an wing elliptical and the objective to minimize the induced drag, research is lead for the use of simple inserted devices perpendicular of the span in the tip-wings known as endplates ([Viieru *et. al*, 2005]). The physical mechanism of the cited device is to minimize the flow that "leak" the tip wing responsible for the vortex generation. These devices are constantly used to increase the efficiency of radio-controlled airmodel used in competitions with the objective to maximize useful load.

Considering the result shown for the lift line theory, we can calculate the enhance of the efficiency in the presence of endplates deducting from the total drag, the drag of pressure or form. Therefore,

$$\Delta C_D = C_D - C_{D,p} = \frac{C_L^2 S}{\pi e b^2}(1 - R) - C_F \frac{S'}{S} \tag{7}$$

where R is a experimental correlation, C_F denote the frictional drag of endplates, $\frac{S'}{S}$ where S' is ratio between the area of the two endplates inserted in the tip wing and its plan area.

By using the experimental correlation (R) propose by Nagel (1924), we can find an expression for ΔC_D of interest for the present theory. The equation can be written in the following form ([Hemke, 1927]):

$$\Delta C_D = \frac{C_L^2 S}{\pi e b^2} \frac{1.66\left(\frac{2h}{b}\right)}{1 + 1.66\left(\frac{2h}{b}\right)} - 2C_F\left(\frac{2h}{b}\right) \tag{8}$$

where $2h$ is the length of the endplate and b is the span of the wing.

It is important to notice from the equation (8), that the drag reduction depends on geometric parameters endplates and its frictional coefficient (C_F). These parameters depends directly on the geometry of the device and the Reynolds number of flow. The equation (8) can also show that the devices have efficiency in cases where the terms on the left hand side (it analyzes the calculation of the induced drag for wing with endplate) surpass the frictional drag generated by devices. This fact show that effectiveness is function of the lift wing and the geometry of endplate. In the present work, experimental results were carried out with different geometries and compared with these theory.

3. THE GURNEY FLAP AND POLYMER SOLUTION

The Gurney Flap was derived from cars of race in the decade of 70, where the pilot Dan Gurney first used it during a test for the modification in the structure of the car. Test had shown excellent aerodynamic efficiency with a considerable increase of the negative lift of the airfoil one by using this device.

The agreement in the enhance of the aerodynamic efficiency in the aeronautical industry was investigated by Liebeck (1970). The same it hypothesized that the trailing would have a previous region with a recirculation and the other region after the flap with two contra-rotating vortices. This fact realize a local effect in the flow field and it modifies the aerofoil geometry in the trailing edge ([Grant, 2006]). The presence of this wake change the stagnation point for a region for out and below of the trailing edge aerofoil, thus increasing the effective chord of the aerofoil (see Fig. 2).

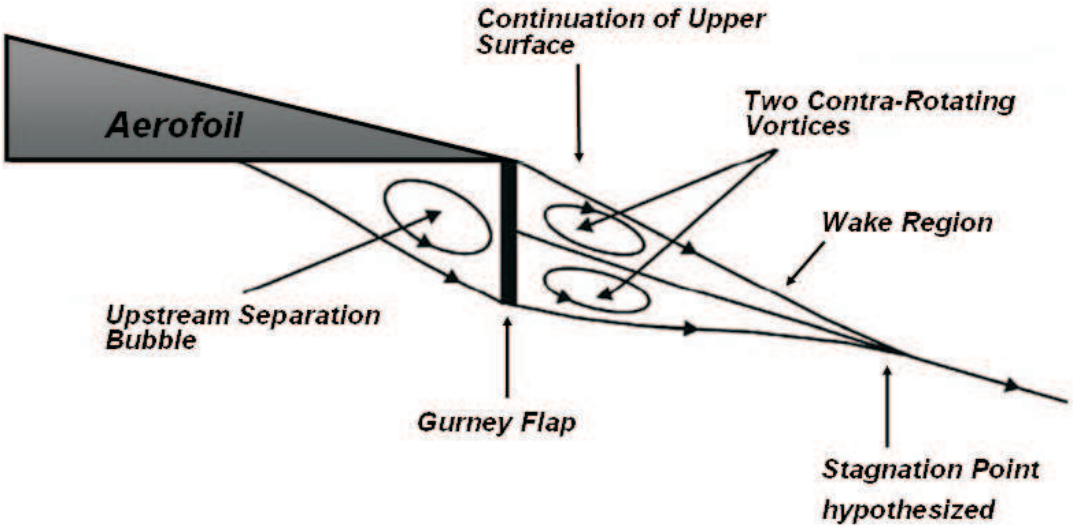

Figure 2. Sketch of the flow in the Trailing-edge by using Gurney Flap in aerofoil.

This fact results in a low pressure region in the wake, and moreover it reduces the adverse gradient pressure around the trailing edge of the aerofoil. Being thus, the separate region in the upper surface satisfactorily is been late or in some cases eliminated and boundary layer thickness also is reduced. The vortices also lead to an increase of the velocity in the upper surface of the aerofoil, so that the region of suction in the trailing edge is increased. In the region of previous recirculation to the Gurney Flap, the flow is decelerated, then in the low surface occurs an increase of pressure in the neighborhoods of the trailing edge. The general effect of increment of suction in the upper surface ally with the increment of pressure in the low surface, takes an increment of the total circulation in the surface of the aerofoil, thus increasing the lift ([Wang and Li, 2002]).

Few studies have been being realized by using polymer solution for reducing drag, however the physical mechanism is not well understood by the scientific way being until the present a theme time of debate. The anisotropy existing due to extension of polymers versus the molecule elasticity in the phenomenon of the drag reduction show some controversy. For the present paper the phenomenon will be described based on works carried out through in internal flows ([Andreotti, 2004]).

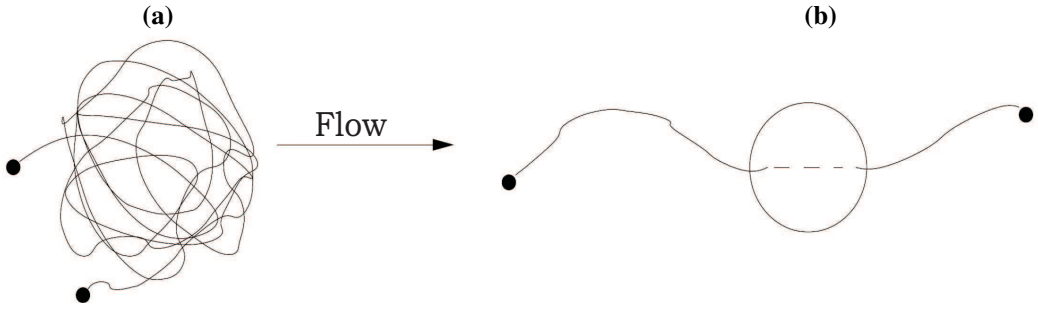

Figure 3. Schematic representation of a polyacrylamide macromolecule. (a) Macromolecule in dynamic equilibrium by the Brownian movement. (b) Macromolecule stretching by the turbulent flow, as a spring.

The mechanism of drag reduction is characterized by the use of small volumetric polymer fractions with anisotropic properties in the fluid. Studies argue that these additives cause one anisotropy in the stress tensor of the flow, reducing efficiency of the momentum transport by turbulent velocity fluctuations of this flow that are responsible for the production of the turbulent energy. This fact will possibly result in the reduction and stabilization of the wake formed in the external flows, that it will make possible in the drag reduction form or pressure for the inserted aerodynamic bodies in this way.

It can be noticed that in the presence of the flow, the distribution of polymers will be affected by the local gradient velocity. This local gradient velocity acting on the polymer will cause an stretching of the molecule (see Fig. 3). This generated stretching is opposing to the Brownian movement that tends to restore the distribution in balance of molecules. In this dynamic balance, the elastic force Brownian, $F_b \sim |r|KT/(N\delta^2)$, where K is the constant of Boltzmann, T is the absolute temperature and $|r|$ is in the distance average of the ends of the molecules, is of the same order of magnitude of the frictional force (Stokes law), $F_v \sim |r|^2(6\pi\mu)/\tau$. Thus, a typical scale of time is of the order of the necessary time that the macro-molecule stretch for the flow restores its equilibrium configuration. Consequently, the relaxation time of an extended polymer to the randomly-coiled state is estimated as being ([Cunha and Andreotti, 2007]):

$$\tau \sim \frac{6\pi\mu\delta^3}{KT}\left(\frac{M}{M_i}\right)^{\frac{3}{2}} \tag{9}$$

where M is the molecular weight of polymer, M_i is the weight molecular of monomer, δ length of the rigid segments of the molecule and μ is the viscosity of the solvent. It is important to notice that the efficiency of these resources just occur in cases in which the relaxation time of polymer be greater than the flow time, being therefore viable in turbulent flows. The aim of this paper will be also show visualizations flow carried out around different geometries by using a hydrogen bubble in presence of polyacrylamide polymer solution.

4. EXPERIMENTAL SETUP

The experiments were carried out in a subsonic wind tunnel, low turbulence ($\sim 1\%$) installed in the laboratory of Fluid Mechanic in the University of Brasilia (see Fig 4). This tunnel have a open-jet with constant total pressure and moderate bands Reynolds number (typically around 10^5), based on model wing chord. The working section have a square shaped of 460 mm x 460 mm and a maximum continuous wind velocity around 20 $\frac{m}{s}$. In order to measure the aerodynamic coefficients was connected to the wind tunnel a balance with three points for measuring the ortogonal and parallel components forces. Measurements these caught by means of the load cells deformations as illustrated in Fig. (4) with electric strain gauges of resistance.

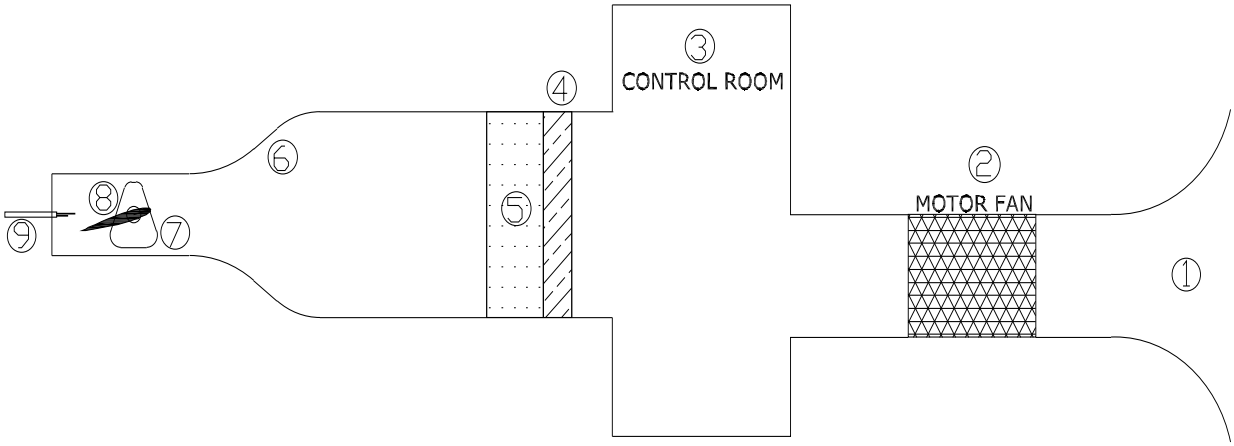

Figure 4. Sketch of the experimental set-up. 1: Incoming Section; 2: Motor Fan; 3: Control Room; 4: Honeycomb; 5: Nylon grid; 6: Smooth contraction; 7: Balance with load cells; 8: Airfoils used to experiments; 9: Pitot tube.

A system of flow visualization hydrodynamics was used to investigate changing in flow structure by adding polymer solution. The polymer on mixed with water by the flow. To carried out the visualizations were injected into the fluid plyolite particles to be convected. To illuminate the apparatus a vertical structure with a reflector was used. The particles reflect the light emitted. The images were recording by using a camera Sony Cyber-shot with a resolution of 4.0 megapixel.

4.1 The model Wings

The model wing was installed horizontally in the test section using a mount where the axis in $\frac{1}{4}$ chord is fixed in the balance of three points with load cells. These configurations permit various freedom degrees necessary for measure lift,

drag and pitching moment of the aerofoils.

The bidimensional geometries used for this work was the no cambered NACA 0012 with 152.4 mm and the aerofoil EPPLER 423 with maximum camber 9,92 % and chord of 189 mm , being this aerofoil considered of high aerodynamic efficiency. Therefore it supplies to high lift and low drag as presented in Fig. (5.a). Both the geometries tested were used in order to compare the experimental measurements with the computacional simulations results of the bidimensional Panel methods.

With the gave to test the enhance of the aerodynamic efficiency by means of high-lift devices was used the aerofoil NACA 2412 with chord of 152.4 mm (see Fig. (5.b)). The device of flap (airfoil additional inserted in the leading edge of the main aerofoil) has 30 % of the main chord and a distance of the 5 % c.

(a) **(b)**

Figure 5. (a) EPPLER 423 aerofoil; (b) Aerofoil NACA 2412 with the plain flap configuration.

A geometric device was used in the NACA 0012 aerofoil known with the Gurney flap. The main goal was a modification in the aerodynamic coefficients and consequently enhance in the aerodynamic efficiency . This device was used in the trailing edge fixed on low surface. Figure (6) shows details of the assembly of the device and the configuration used in the experiments. The Gurney flaps were made of aluminum alloy, 0.8mm in thickness, spanning the whole span of the tested airfoil.

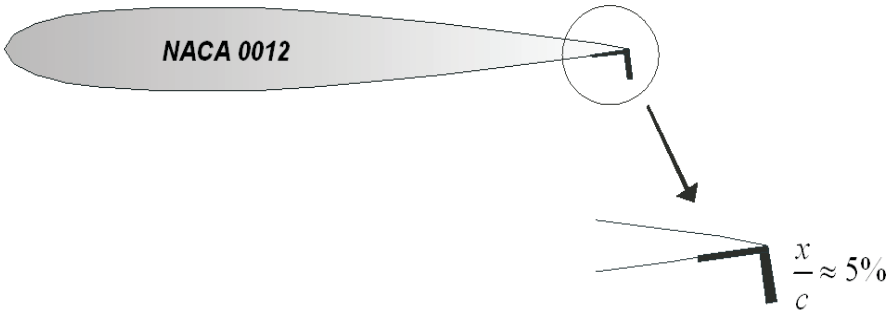

Figure 6. Sketch of the NACA 0012 aerofoil section with the Gurney Flap.

In addition, experiments were carried out with wing un-tapered and aerodynamics untwisted NACA 0012 aerofoil.

(a) **(b)**

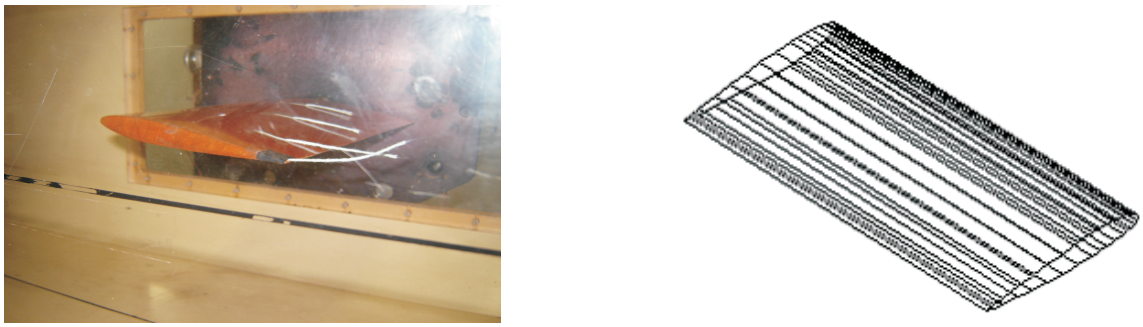

Figure 7. (a) The wing with NACA 0012 aerofoil section used in wind tunnel; (b) Tridimensional Geometric of the NACA 0012 aerofoil section.

The model chord length was 152.4 mm with spans giving aspect ratios of two and four. Figure (7.a) shows details of the wing during an experimental in the wind tunnel. In addition, experiments were carried out with three different configurations endplates for these wings.

5. RESULTS AND ANALYSIS

Considering the methodology used, the experimental error bars associated with the aerodynamics coefficients measurements are calculated based on a analysis of uncertentainty discussed in [Cunha *et. al*, 1997]. In order to understand the flow with additives experiments had been carried through an aerodynamic body in form of losango and a polyacrylamide solution of 300 ppm, where this ratio in volume reduced approximately in 64 % of the drag of internal flow ([Cunha and Andreotti, 2007]). The main objetive will be understand the differences in the instantaneous wake with and without the effect of the additives. Figure (8) presents the experimental results of visualization of the flow field. We can see that the use of polymer in flow results in the reduction of the oscillation generated in the wake and the intensity of vorticity, supplying thus one better stabilization of this downstream body. This fact show the importance of the macromolecules on the flow. Actually, the intense gradients of velocity of the wake is damping by elasticity and anisotropy of the polyacrylamide molecule. This phenomena contributes to reduce turbulent fluctuations of the flow. Another characteristic also observed is that occurred a reduction of the amplitude of the oscillation. Possibly it result in the drag pressure reduction. Future works will be carried out to measurements of aerodynamics coefficients of the body and realize a stochastic analysis of flow response to quantify the differences.

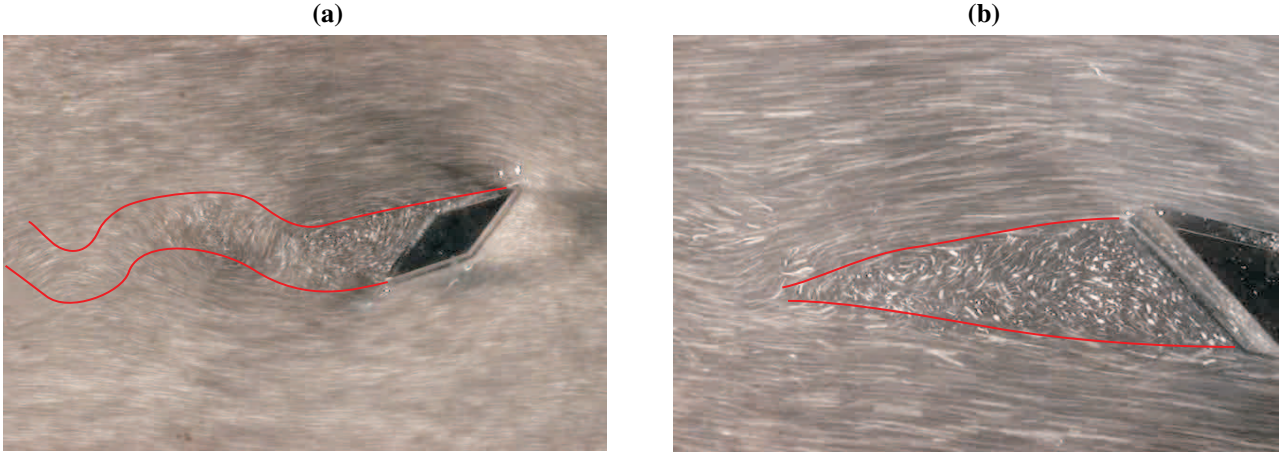

Figure 8. Flow visualization of aerodynamic body by using polymer solution of poliacrilamide (a) Case with no solution of PAMA; (b) Case with solution of PAMA.

In order to understand the differences between the geometric parameters was conducted first the influence on the flow of camber in aerofoils. The experimental results was investigated with the bidimensional panel method to verify the accuracy of the boundary integral code developed. Figure 9 shows the lift coefficient for several attack angles and compares a aerofoil cambered without cambered. The plot shows that the aerofoil cambered have a lift coefficient always greater than the symmetrical aerofoil for all the attacks angle. The increasing was approximately 77 % for the maximum lift coefficient and its angle of stall increased for 14 degrees. This is superior in 4 degrees when compared with the aerofoil NACA 0012. The best linear fit was $C_L \cong 0.109\alpha$ for NACA 0012 aerofoil and $C_L \cong 0.091\alpha + 1.02$ for the cambered aerofoil, in which its inclination are approximately that proposal for the thin aerofoil theory $\pi^2/90$ ([Anderson, 1991]). It is seen that an attack angle, the predictions of the bidimensional Panel methods agree well with the experimental measurements, with a difference less than 20 % for the cambered aerofoil,that occur due the high thickness and wake generated in trailing edge.

In addition, we realized experiments to verify the influence of the high-lift device. Figure 10 show results of lift coefficients to the NACA 2412 aerofoil with plain flap for several angles. The experimental results were compared with the numerical predictions using the bidimensional panel methods. We can see that the variation of the flap angle increase the lift coefficient for all angle of attack and its intersection in the ordinate axis. This fact show that the curve suffer a positive displacement throughout the ordinate axis and its inclination keeps approximately constant until 30^o of flap angle. Being thus, the global result will be a considerable enhance of the lift. For a flap angle of 45^o was verified an average increasing of 93 % in the maximum lift coefficient. Figure (10.b) show that for flap attack angles until 15^o the predictions given by the panel method is in a good agreement with the experimental measurements. Its seen the divergence for angles greater because is not predicted by the method the boundary layer separation.

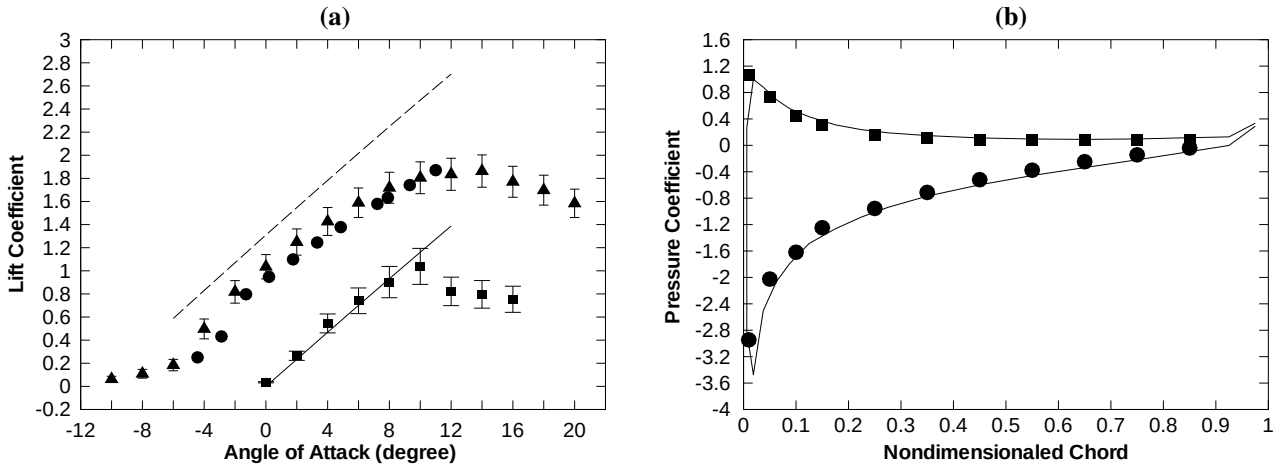

Figure 9. (a) Lift Coefficient for different aerofoils. The continuous and dashed line represents the predictions of the bidimensional panel method, respectively. The box represents the experimental measurements of the NACA 0012; The triangle represents the experimental measurements of the EPPLER 423 compared with UIUC Airfoil Data Site represented by the circle; (b) Pressure distribution for the NACA 0012. The symbols represents the experimental results and continuous line the numerical simulation; The Reynolds numbers of the experiments was 2 x 10^5.

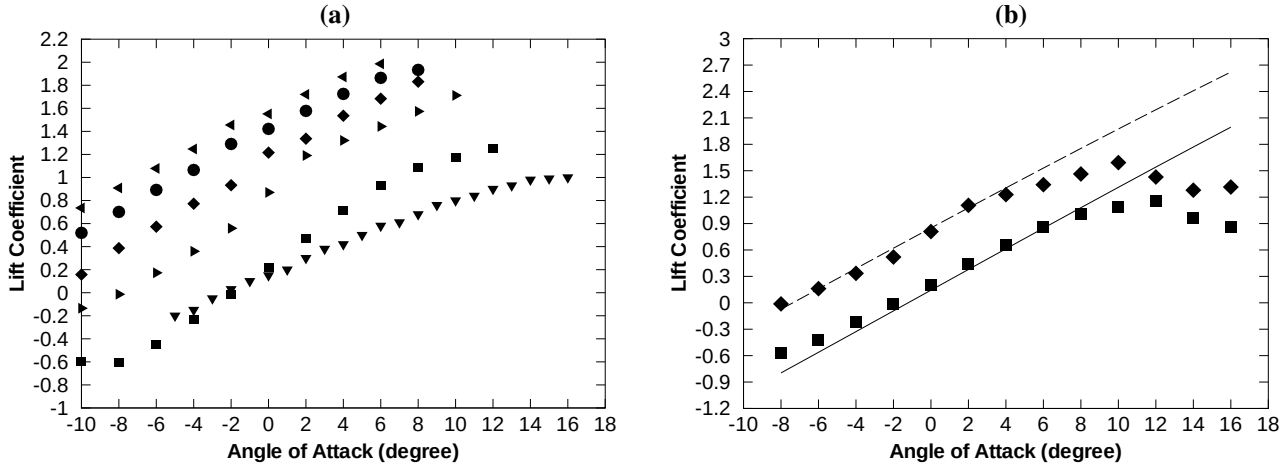

Figure 10. (a) Lift Coefficient for NACA 2412 aerofoil with plain flap. The gradients represents a NACA 2412 aerofoil with no flap; The square, right triangle, diamond, circle and left triangle represents the flap angle 0^o,15^o,30^o,45^o,60^o, respectively. (b) The solid and dashed line represents the predictions of the bidimensional panel method for flap angle 0^o and 15^o, respectively. The symbols represents the experimental results; The Reynolds numbers was 2 x 10^5.

Another application of the high-lift device was to explore the influence of gurney flap in no camber aerofoil. Figure (11) shows a experimental result for lift coefficient versus drag coefficient for several attack angles .In addition, the pressure coefficient as a function of the dimensionless chord is shown in figure (6). We can see that on the presence of Gurney Flap lead to substantial increase of the lift coefficient of global for all the angle of attacks. The maximum lift coefficient were of 1.54 for an angle of 8^o and zero lift for angle of attack -6^o, while for the aerofoil without the device the maximum lift coefficient was of 0.835 for an angle of 10^o. These results indicates that the gurney flap insert a "pseudo" camber in the geometry. Figure (11.b) shows an increase the suction in upper surface. On the order hand in the lower surface an increase of the pressure in neighborhoods of the device is observed because the flow was decelerated. These phenomena results in a direct enhance on the difference of the pressure between lower and upper surface that change to the drag coefficient of 0.03 gets a lift coefficient of 1.1 and 0.4 for a aerofoil with and without Gurney Flap, respectively.

Figure (12) shows the predictions of the lift line theory for the lift coefficient and for the induced drag coefficient in comparison with experimental results for a wing with NACA 0012 aerofoil section for different aspect ratios. Its is seen a reduction of slope of the curves with the decrease of the aspect ratio. The linear fits were of $C_L \cong 0.084\alpha$ and $C_L \cong 0.046\alpha$ for aspect ratio of 4 and 2, respectively. Its important to note that the slopes were smaller than that corresponding to one for two-dimensional potential flow around a thin aerofoil.

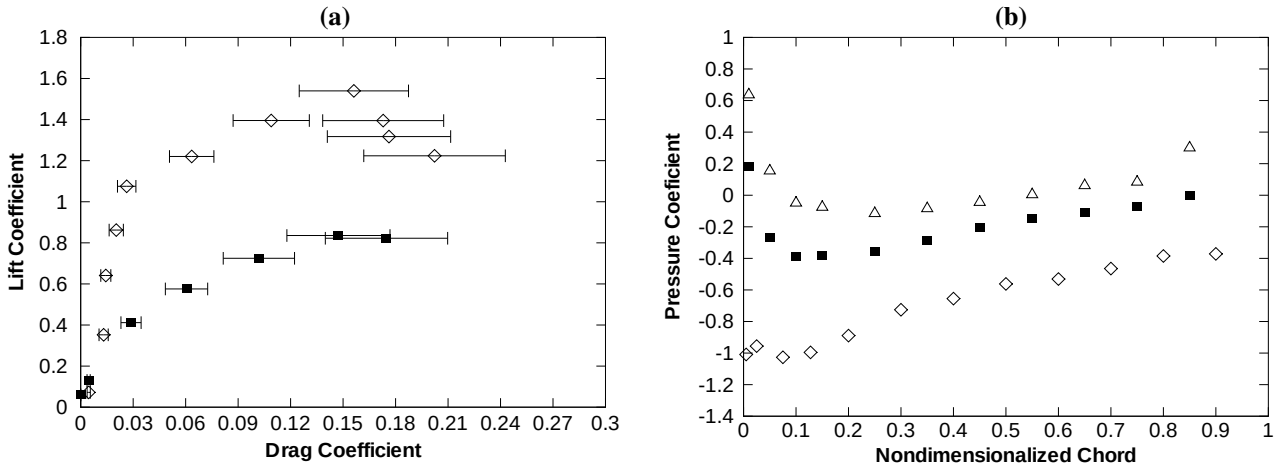

Figure 11. Polar curves and pressure coefficient for NACA 0012 aerofoil with gurney flap. (a) The diamond and box symbols represents the aerofoil with and in the absence of gurney flap, respectively. (b) The no filled symbols represents the aerofoil with gurney flap for attack angle 0^o. The Reynolds number was 2.0 x 10^5

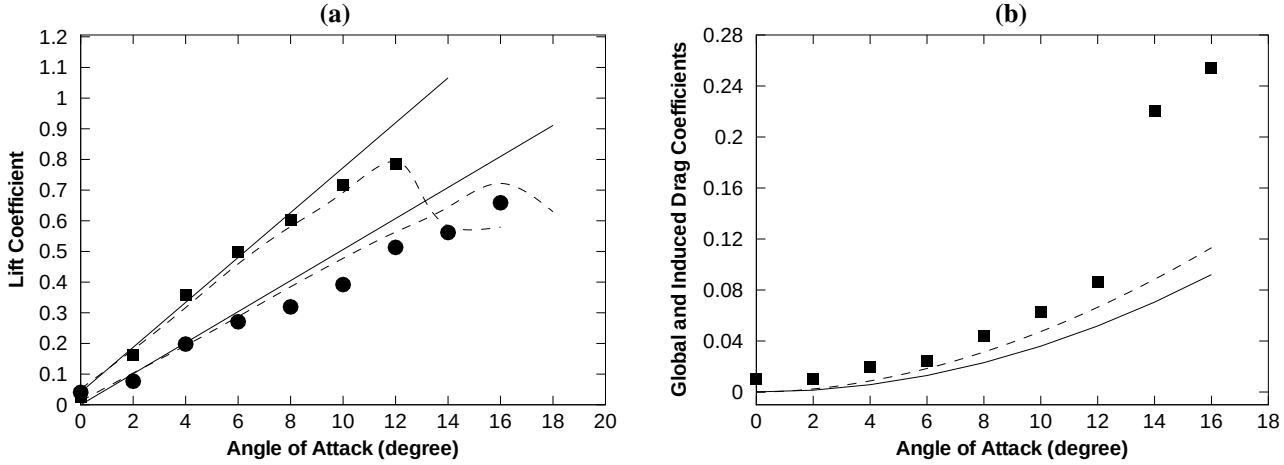

Figure 12. Lift coefficient, drag coefficient and induced drag coefficient for a wing with a NACA 0012 aerofoil. The continuous line represents the predictions of the lift line theory linear and the dashed line represents the predictions of the lifting-line theory nonlinear. the square and circle symbols represents the experimental results for the aerofoil with 4 and 2 aspect ratio, respectively. The Reynolds number of the experiments was 2.0 x 10^5

In addition to reduction of the maximum lift coefficient its seen that occurs an increase in the stall angle with the decrease of the aspect ratio, being approximately 12^o and 16^o for aspect ratio of 4 and 2, respectively. This finding is quite common for flows around finite wings, because occurs an increase of the induced angle with reduction of the aspect ratio. We can also see that for angles of attack below the stall, the predictions of lift line theory agree very well with the experimental measurements. The discrepancy occurs in view of that the viscous forces that has not been accounted by the theory. However, with the results predicted to the lift-line theory nonlinear was possible to predict the angle of stall, because the calculation is carried using the curve (C_L vs. α) of the aerofoil. The predictions given by this method showed that the induced drag coefficient has a contribution of the total drag coefficient of approximately 70 % and 60% for aspect ratio of 2 and 4, respectively.

In order to reduce the induced drag of a wing with NACA 0012 aerofoil section was tested for different geometries of endplates. The figure (13) presents experimental measurements of the lift coefficient and drag coefficient for several attack angles.

The experimental results pointed out that both aspect ratio, the classic geometric of endplates reduced the global drag due diminishes the induced drag. Comparing the plots, we can see that the aspect ratio 2, the geometries showed very good efficiency reducing the induced drag for almost all lift coefficients. However, for aspect ratio 4 the efficiency was observed only to high lift coefficient. Then, this device recommended to high Reynolds flow for lower aspect ratio, where the tip vortex has a stronger effect ([Viieru *et. al*, 2005]). This behavior is see from experimental observation in the wing with aspect ratio of 2. The table (1) shows a comparison between experimental results and the correlation predicted in this work for aspect ratio 2. The values of C_F used for geometry elliptical and circular have been 0.014 and for trapezoidal

0.008 ([Hemke, 1927]). These values are used as being recommendable in the literature, considering that in the present work these coefficient were not calculated for the effective experimental conditions.

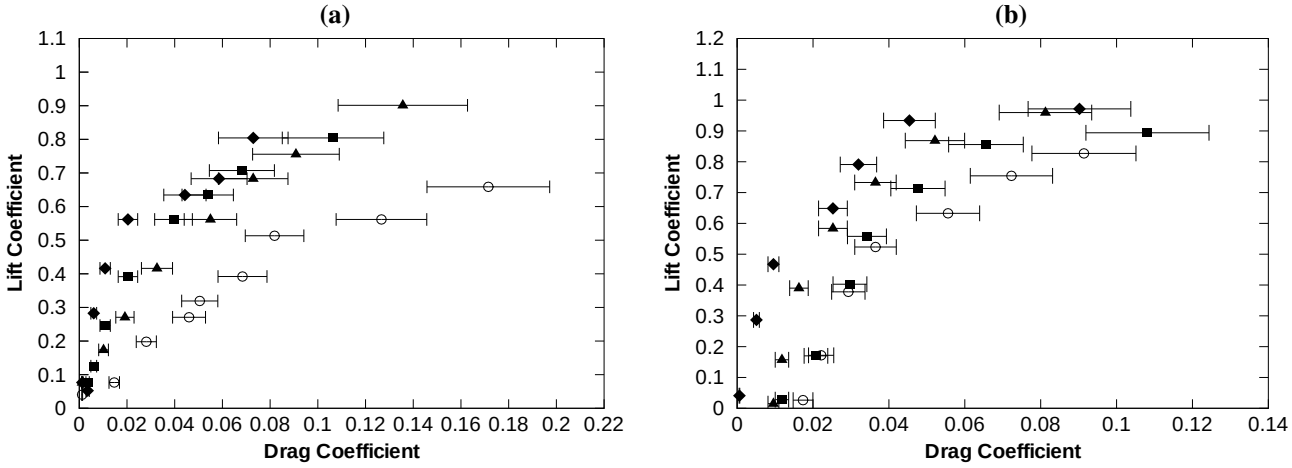

Figure 13. Polar curves for wing with NACA 0012 aerofoil and three configuration of the endplates. The diamond, triangle and square represents the wing with trapezoidal, circular and elliptic endplate, respectively. The circle no filled represents the wing in the absence endplate (a) The experimental results of the wing with aspect ratio of 2; (b) The experimental results of the wing with aspect ratio of 4. The Reynolds number of the experiments was 2.0 x 10^5.

Table 1. Reduction of induced drag C_{Di} for theoretical prediction pre showed and experiments for different geometries endplates.

Aspect Ratio	Endplate geometry	Experimental Red [%]	Correlation Red [%]
2	elliptical	53	74
	Circular	32	66
	trapezoidal	50	68

The investigation have shown that the device tested reduce induced drag, but the values of the theoretical prediction were greater than experimental results. The divergence occurred because the real friction coefficient used is not same with that adopted by this work. Another point that justify the discrepancy is the fact of the reduction be based on the global drag and the correlation was calculated only the induced drag.

Another device that modify the aerodynamics coefficients is the tapered wing. The figure (14) shows predictions of the lift-line theory for the lift coefficient and for the induced drag coefficient throughout the semi-span with a cambered aerofoil section. We can see that with the taper ratio occurs an increasing of distribution of the lift coefficient between 10% and 40% of the semi-span and changing to the zero in the tip of the wing. Actually, modification of the lift distribution area results in an increase of the global lift coefficient. The numerical results show in particular that the taper ratio reduces the induced drag coefficient in the neighborhoods of the central region semi-span and displacement of the maximum coefficient drag to the tip of the wing. Consequently, this distribution will reduce the global induced drag coefficient. For the taper ratio of 0.4 the efficiency of the wing increased of 42.5 % when compared with a wing no tapered, being this case common in reduced scale aircraft.

In addition, a simulation with three-dimensional potential boundary integral method was explored for evaluation of forces coefficients for a wing swept, with out tapered and no twist. The aerofoil section used was a SELIG 1223 for all span and the number of grid elements that represented the surface of the wing was 1440. This mesh was sufficient to give accurate the results as shown in the work realized by Alvarenga and Cunha (2006). The Figure (15) shows a comparison between those wing swept back and swept front with angle of attack of 5^o. This plot shows that the use of swept front generate a lift reduction throughout the wing including the tips when compared with a wing no swept. Then, this phenomena certainly will contribute to reduce the global lift. However, with the induced drag was seen a reduction for all span, resulting an a direct decreasing global induced drag. For a swept back wing occurred a decreasing of lift distribution along of the center of the span and the tip almost not had difference. The induced drag distribution reduces in the tip and enhance in the center of the span. Then, this geometric parameter has a function in the control of streamline deviation produced in flow around of the wing, effect that is responsible in modifying the pressure field. Table (2) gives the aerodynamics coefficients obtained for each wing configuration.

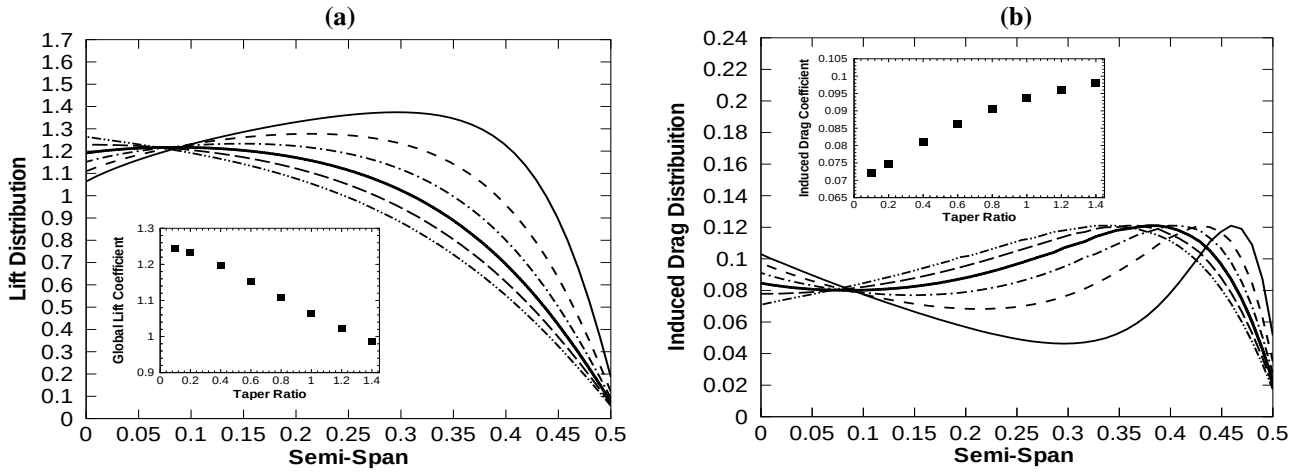

Figure 14. Forces coefficients for an tapered wing. The continuous, dashed, dashed-dot, dotted, long-dashed and dashed dot-dot represents the predictions of the lift line theory for 0.2, 0.4, 0.6, 0.8, 1.0, 1.2, respectively. (a) Distribution of lift coefficient; (b) Distribution of induced drag coefficient.

The results have shown that a swepted wing enhance the performance of the wing, as a consequence of the reduction on the induced drag is rather than an increasing on the global lift. So, this geometric device is a excellent way to optimize a project of a aircraft. For the case of this work, specifically, the wing with back swept has presented a bigger efficiency than the one with front swept.In fact, it just confirms the importance use of this geometry in various aircraft that flying subsonic regime. Finally, it should be important to note that the angle of swept is an essential parameter to project the aircraft, but for the back swept the pitching moment coefficient turned negative differently of the other case.

Table 2. Results of aerodynamics coefficients obtained from Boundary integral methods for swept wing with SELIG 1223 aerofoil section.

Swept	C_L	C_D	C_m pitching	C_L/C_D
-45	1.209	0.0802	0.7189	15.1
0	1.4617	0.1153	-0.691	12.6
45	1.1809	0.0636	-1.9573	18.6

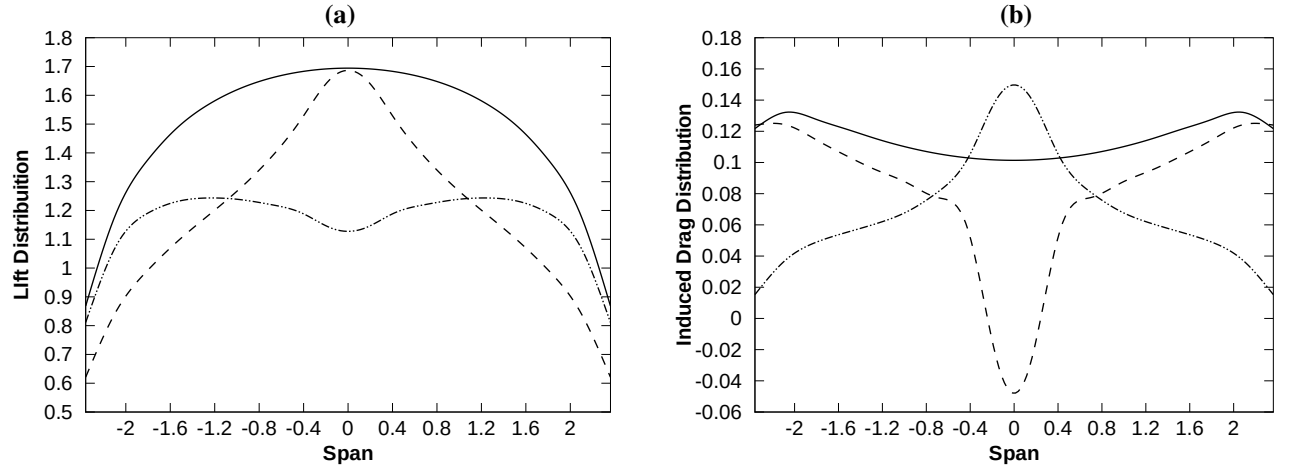

Figure 15. Lift coefficient and Induced drag coefficient distributions for a swept wing. The dashed, continuous and dash-dotted represents the predictions from Boundary integral methods of the -45^o, 0^o and 45^o swept, respectively. (a) Distribution of lift coefficient; (b) Distribution of induced drag coefficient.

6. CONCLUSION

In this paper we have presented experimental and numerical results based on the potencial theory using geometric devices that modify the aerodynamics coefficients. The drag and lift study has shown that when using the camber and

high-lift devices it is possible to enhance these quantities and realize a study of the aerodynamic performance of the aerofoil. Especially, was observed that the gurney flap obtained aerodynamics coefficients of cambered aerofoil, showing extremely important to aircraft design due to the have low cost implementation. The visualization of flow when adding polymer solution produced a stabilization and a reduction of wake instabilities, showing that is necessary to deep study in future research. For wings, was seen that the aeronautic project have several factors that have influence in aerodynamics coefficients. The reduction of the aspect ratio modified the maximum lift and stall angle and the use of taper ratio enhanced the aerodynamics efficiency. One important conclusion from the experimental observation that the methodology was coherent because the data compared with the literature showed very good agreement. To control the induced drag all geometries endplate have shown positive results, especially for low aspect ratio. The numerical description was carried out using the panel methods for two-dimensional flows, the lift-line theory and the boundary integral method to three-dimensional potential flows. The low computing cost and high accuracy with the experimental results for all methods makes it attractive to apply the potencial theory for high Reynolds flow, in particular aircraft design.

7. REFERENCES

Alvarenga, R. C., Cunha, F. R., 2006, " Boundary Integral Simulations of Three-Dimensional Inviscid Flows", Latim American Journal of Solids and Structure, pp. 161 – 174.

Alvarenga, R. C., 2000, " Um Estudo de Escoamentos em Altos Números de Reynolds com Aplicação na Aerodinâmica",Relatório de Projeto final , Depatarmento de engenharia Mecânica (Orientador F. R. Cunha) – UnB, 140p.

Anderson, J. D., 1991, " Fundamentals of Aerodynamics ", Mcgraw-Hill higher education, second edition, 772 p.

Andreotti, M., 2004, " Estudo Teórico-Experimental do Fenômeno de Redução do Arrasto de Escoamentos Turbulentos por Adição de Polímeros ", Dissertação de Mestrado, Publicação DM-072, Departamento de Engenharia Mecânica, Universidade de Brasília, Brasília, 154 p.

Carrannanto, P. G., Storms, B. L., Ross, J. C., Cumming, R. M., 1998, " Navier-Stokes Analyses of Lift-Enhancing Tabs on Multi-Element Airfoils ", Aircraft Design, pp. 145–158.

Cunha, F. R., Andreotti, M. A., 2007, "A Study of the Effect of Polymer Solution in Promoting Friction Reduction in Turbulent Channel Flow ", Journal od Fluids Engineering.

Cunha, F. R., Souza, A. J., Rodrigues, J. L. F. e Solomom, L. R., 1997, " Uma investigação Experimental da Ação Estática do Vento sobre uma Torre de Geometria Complexa ", Revista Ciência e Tecnologia 6(1): 40–49.

Grant, I.,McCutcheon, G.,McColgan, A. H.,Hurst, D., 2006, " Optical-velocimetry, wake measurements of lift and induced drag on a wing ", Optics and Lasers in Engineering, No. 44, pp. 282–303.

Henke, P. E., 1927, " Drag of wings with endplates ", Langley Memorial Aeronautical Laboratory, Report No. 267.

Jang, C. S., Ross, J. C. and Cummings, R. M., 1998, " Numerical investigation of an airfoil with a gurney flap ", Aircraft Design , No. 1, 75.

Li, Y. C., Wang, J. J., Tan, G. K., Zhang, P. F., 2002, " Effects of gurney flaps on the lift enhancement of cropped nonslender delta wing ", Experiments in fluids 32, pp. 99–105.

Li, Y. C., Wang, J. J., Zhang, P. F., 2002, " Effects of Gurney Flap on NACA 0012 Airfoil ", Flow, Turbulence and Combustion, No. 68, pp. 27–39.

Liebeck, R. H., 1970, " Optimization of Airfoils for Maximum Lift ", Journal of Aircraft, 409.

Nagel, F., 1924, " Flügel mit seitlichen Scheiben ", Vorlaufige Mitteilungen der Aerodynamischen Versuchsansalt zu Göttingen, N o.2.

Resende, O. C., 2004, " The Evolution of the Aerodynamic Design Tools and Transport of Aircraft Wings at Embraer ",J. of Braz. Soc. of Mech. Sci. and Eng, 26, 379.

UIUC Airfoil Data Site, Michael Selig, " Department of Aeronautical and Astronautical Engineering ", University of Illinois at Urbana-Champaign, Urbana, Illinois 61801.
http://amber.aae.uiuc.edu/m-selig/ads.html

Viieru, D., Albertany, R., Shyy, W., and Ifju, G. P.," Effect of Tip Vortex on Wing Aerodynamics of Micro Air Vehicles ", Journal of Aircraft, Vol. 42, No. 6.

Wang, J. J.,Li, Y. C., 2002, " Experimental investigations on the mechanism of gurney flaps lift-Enhancement ", The Polytechnic University of Hong kong, People's Republic of China.

8. Responsibility notice

The authors Rafael Paulino de Queiroz, Ricardo Caiado Alvarenga and Francisco Ricardo Cunha are the only responsible for the printed material included in this paper.